Optics Communications 282 (2009) 2023–2027

Contents lists available at ScienceDirect

Optics Communications

journal homepage: www.elsevier.com/locate/optcom

Enhanced transmission of light through periodic and chirped lattices of nanoholes

Alexander Minovich [a,*], Haroldo T. Hattori [b,c], Ian McKerracher [b], Hark Hoe Tan [b], Dragomir N. Neshev [a], Chennupati Jagadish [b], Yuri S. Kivshar [a]

[a] Nonlinear Physics Centre, Research School of Physics and Engineering, Australian National University, Canberra, ACT 0200, Australia
[b] Department of Electronic Material Engineering, Research School of Physics and Engineering, Australian National University, Canberra ACT 0200, Australia
[c] School of Information Technology and Electrical Engineering, University of New South Wales, The Australian Defence Force Academy, Canberra ACT 2600, Australia

ARTICLE INFO

Article history:
Received 13 November 2008
Received in revised form 12 January 2009
Accepted 12 January 2009

ABSTRACT

We study experimentally the transmission of light through periodic and chirped lattices of nanoholes perforated in an optically-thick gold film. We observe that the periodicity of the structure enhances the light transmission for specific wavelengths, and we analyze this effect theoretically by employing finite-difference time-domain numerical simulations. Furthermore, we demonstrate experimentally the possibilities for manipulation of the spectral transmission in quasi-periodic and chirped lattices consisting of square nanoholes with varying hole size or lattice periodicity.

1. Introduction

The recent studies of light transmission through sub-wavelength apertures [1] was triggered by the discovery of extraordinary transmission of light through periodic arrays of nanoholes [2,3]. For more than a decade the nature and magnitude of the observed transmission enhancement has been studied in a number of works both theoretically [4–24] and experimentally [25–36]. A large part of these studies have been dedicated to the role of surface plasmons in this extraordinary transmission [15,16,19,25–27,29,35,36]. While the contribution of surface plasmons in the enhanced transmission through perforated metal films as well as the amount of enhancement of the light transition through the film can be argued [36], it is important to note that surface corrugations of the metallic films provide an efficient mean for excitation of surface plasmons.

The enhanced transmission of light appears exceptionally promising for novel photonic applications [39], including spectral filters and photon sorters [38], however, the most exciting opportunity comes from the fact that surface plasmons can provide high-intensity fields near the metal surface. The plasmonic field enhancement has proven beneficial for precision optical manipulation of nanoparticles [40], surface enhanced Raman scattering [41], plasmon-enhanced high-harmonic generation [42], and nonlinear optical bistability [43,44].

Optical bistability arises due to the strong dependance of optical transmission on the refractive index of the substrate. The bistable behavior is determined by the metal properties as well as by the structural parameters of the perforated film [45,46]. The nonlinear change of any of these parameters at high light intensities can thus provide a mechanism for all-optical manipulation of light. Importantly, such nonlinear change of the transmission can happen at laser powers of just a few mili-Watts [44], therefore opening novel applications for low-power all-optical switching.

Despite the demonstrated results on nonlinear control of transmission in nanostructured metallic films [44,47], the field still requires further advances in the order to enhance the nonlinear response of the structures. For this purpose, an important task is the design and optimisation of the parameters of the perforated films. The main task of such design is to achieve narrow transmission resonances enabling strong nonlinear effects at lower light powers.

In this paper we study, both theoretically and experimentally, the transmission properties of gold films perforated with square sub-wavelength apertures in different arrangements. We show how the periodical arrangement of the nanoholes can enhance collective plasmonic resonances in the metal film. We analyze our experimental observation by employing numerical simulations based on the finite-difference time-domain (FDTD) approach. Furthermore, we explore several ways to design the transmission through perforated metal films by introducing quasi-periodicity or aperture size chirping.

The paper is organised as follows. In Section 2 we discuss our experimental setup and summarize our experimental results. Section 3 is devoted to our numerical results and a brief discussion of the numerical methods we used. In Section 4 we study two new geometries of the nanohole lattices, created by chirping of the square arrays through changing of the hole radius or the lattice spacing. Finally, Section 5 concludes the paper.

2. Experimental studies

For fabrication of our samples we use a focused ion beam (FIB) milling system to drill nanoholes in a 200 nm thick gold film. The

* Corresponding author.
E-mail address: min124@rsphysse.anu.edu.au (A. Minovich).

0030-4018/$ - see front matter © 2009 Elsevier B.V. All rights reserved.
doi:10.1016/j.optcom.2009.01.060

gold film is deposited on top of a quartz substrate using DC magnetron sputtering in an Ar ambient. Four different sample geometries are fabricated and tested. The first two geometries represent square hole homogeneous lattices of 40×40 holes with spacing of 2 μm between them and a hole size of 800 and 300 nm, respectively. The other two samples represent somewhat the more complex geometries of Thue–Morse sequence of holes and chirped size hole lattice, respectively.

We characterize the spectral transmission of these samples by employing the experimental setup shown in Fig. 1. We use a supercontinuum radiation generated by focusing of 140 fs pulses at 0.8 μm wavelength in a photonic crystal fibre with a zero dispersion wavelength at 0.74 μm. The supercontinuum spectrum spans over the wavelength range 0.45 – 1.7 μm enabling transmission measurements over a broad spectral range. The supercontinuum beam is mildly focused onto the film from the air-gold interface. The illuminated area of the film is 20 μm, being determined by the size of the focal spot on the metal film. The light transmitted through the film is projected with a microscope objective on a CCD camera for identification of the perforated areas and analyzed by an optical spectrum analyser (OSA) (Agilent 86140B). In order to minimize the influence of possible spectral fluctuations in the supercontinuum source, the output spectra are recorded simultaneously with the spectrum from a reference beam on OSA 1 (Fig. 1). All measurements are normalized to the transmission through a blank quartz substrate.

First we measure the transmission spectra of the two homogeneous arrays consisting of 800 nm and 300 nm wide square holes [see insets in Fig. 2a and b, respectively]. Our measurements are performed in the spectral range of 0.6–1.7 μm that is determined primarily by the range of the OSAs. The measured transmission spectra of both samples are shown in Fig. 2. From the figure, we see that the sample with 800 nm size holes shows, on average, higher transmission than the sample with 300 nm size holes. However, no clear resonance enhancement peaks can be identified in the monitored wavelength range (Fig. 2a). On the contrary, the sample with smaller holes (300 nm) exhibit a number of closely spaced resonances (Fig. 2b). Five resonances are observed in the red and near-infrared range (0.6–1.0 μm) followed by monotonic drop of the transmission in the wavelength range 1.0–1.4 μm. At even longer wavelengths (1.4–1.7 μm) new transmission resonances can be seen. The total transmission, however, remains below 5×10^{-4}.

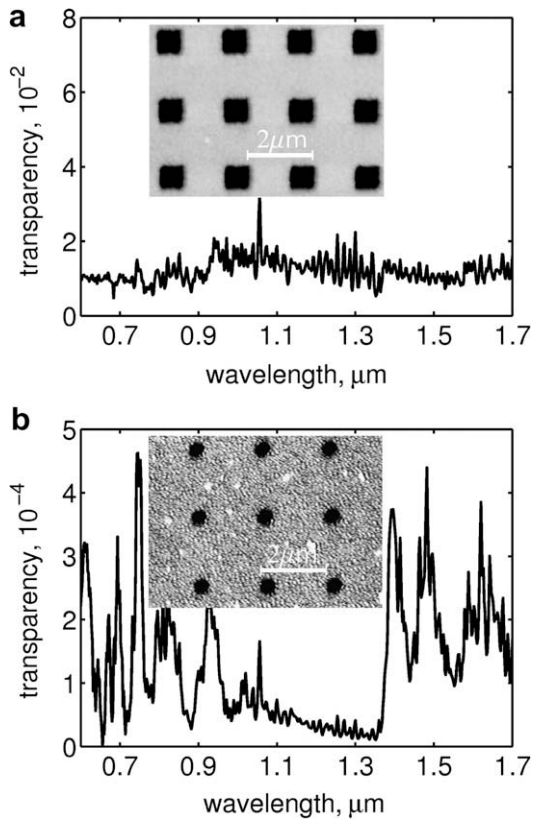

Fig. 2. Normalized transmission spectrum (normal incidence) of homogenous lattice of holes with size of 800 nm (a) and 300 nm (b). Insets – atomic force microscope images of the corresponding hole lattices.

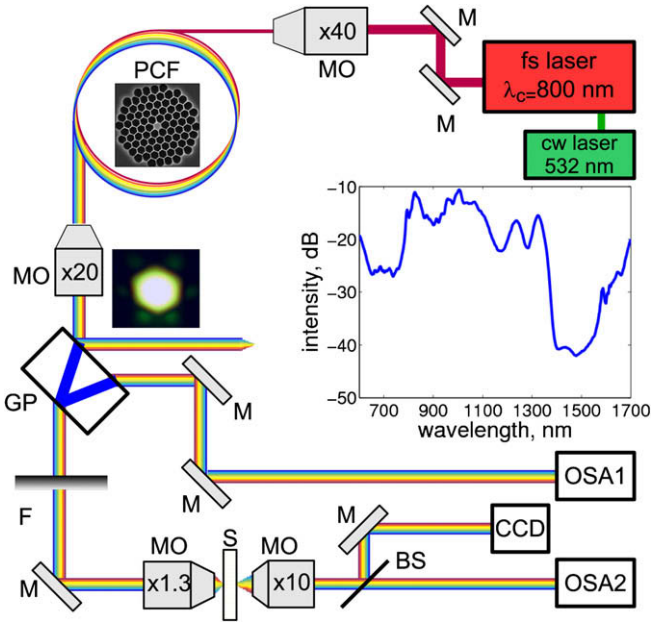

Fig. 1. Experimental setup: M, silver mirrors; MO, microscope objectives; PCF, photonic crystal fibre; GP, glass plate; F, neutral density filter; BS, beam splitter; S, sample; CCD, color camera; OSA, optical spectrum analyzers. Inset – graph of the generated supercontinuum spectrum.

To understand the origin of the observed transmission peaks we resort to numerical calculations of the transmitted spectra. The numerical simulations also enable a direct comparison of the transmission through an array and a single aperture only, allowing to analyse the influence of the periodic arrangement of holes on the excitation of surface wave and surface plasmons.

3. Numerical results

In our FDTD simulations, we excite the sample with a short pulse, broad spectrum source and collect the transmitted power at 3 μm distance from the structure. At this distance, the contribution from the evanescent fields on the output transmission spectrum can be neglected. The frequency content of the transmitted power is then analyzed by utilizing fast Fourier transformation. In our simulations we use a non-uniform grid with size varying from 2 nm near the surface to 20 nm in a free space and a time step cT of 1 nm. To calculate the transmission through a lattice of holes we use a cell containing a single hole only and utilize periodic boundary conditions, while for transmission through a single hole we implement a perfect matching layer at the boundaries.

For the lattice of 800 nm holes, the calculations (Fig. 3a) did not reveal any clear transmission resonances in the visible part of spectrum (apart from the pure gold transmission peak) but showed transmission peaks at infrared wavelengths, at about 1.6, 2.3 and

3.2 μm. This observation is in a qualitative agreement with our experiments, where no distinct resonances were measured in the transmission in the visible and near-infrared regions.

The sample with the lattice of 300 nm holes, on the other hand shows few weak peaks in the wavelength range between 0.6 μm and 1.0 μm, followed by a lack of transmission in the region 1.0–1.3 μm, and some weaker transmission peaks in the 1.5 μm range (Fig. 3b). These characteristic features well match the observed resonance peaks in the experimental data, however, the strength of these resonances differs from the measured quantities. Most likely this is due to imperfections in the fabricated samples, including deviation from the square shape of the holes, surface roughness (see AFM image in Fig. 2b), or residual gold inside the holes.

A comparison of the spectra for a nanoholes lattice (Fig. 3 (solid lines)) and for a single isolated hole (Fig. 3 (dashed line)) show that the observed enhanced transmission peaks are clearly due to a collective effect (excitation of surface waves and/or surface plasmons) due to the periodic arrangement of the nanoholes (Fig. 3). In particular, in the case of holes of 300 nm size, we can see more than six times enhancement of the transmission in a comparison with the light transmitted through a single hole at a wavelength of 0.7 μm. This enhancement is comparable to the theoretically predicted maximum enhancement of the transmission in such lattice of nanoholes [36]. Importantly, the lattice periodicity enables the momentum matching of the incident light to the excited surface waves and electric field enhancement near the gold surface.

The excitation of surface waves can be clearly seen in the example of the electric field distribution calculated for a wavelength of 0.7 μm. Fig. 4a shows the Z component of the electric field after the incident light is coupled to a single square hole of 0.3 μm size. One can see that the field in this case is only concentrated near the edges of the hole. In contrast, in the case of periodic arrangements of holes (Fig. 4b), every hole generates waves which propagate along the metal–air interface, and form a standing interference pattern [37]. This pattern can be clearly seen in Fig. 4b. The wavelength of the excited surface waves, calculated from the distance between the interference peaks, is approximately 0.7 μm, similar to that of the incident light.

We would also like to point out a feature of the transmission spectra which is essential for the experimental characterization and can lead to significant differences between calculations and experimental measurements. Due to the high divergence of the light exiting through a single nanohole [48], the measurement of transmission need to be realised with high numerical aperture (NA) objectives in order to collect as much light as possible from the output face. To demonstrate the importance of the output divergence of the beam exiting from a single aperture, we performed calculations for a single hole transmission when the light is collected by a monitor with NA of 0.8 and 0.2. The results of these simulations are shown in Fig. 3, dashed and dashed dotted line, respectively. As one can see, the NA of the collecting objective can cause not only quantitative but also qualitative changes in the measured transmission spectrum.

Next, we performed a number of simulations in order to investigate the dependence of the transmission on the angle of incidence (Fig. 5). In our simulations, we consider a sample with 800 nm size square holes and calculated the spectral transmission for normal incidence and two other inclination angles. The results show that the inclination of the sample causes significant deformation of the transmission spectrum in the short-wavelength region, leading to lower transmission. The direction of the shift of transmission peaks helps us to determine what phenomenon is related to the correspondent peak. Positive order Wood anomalies and

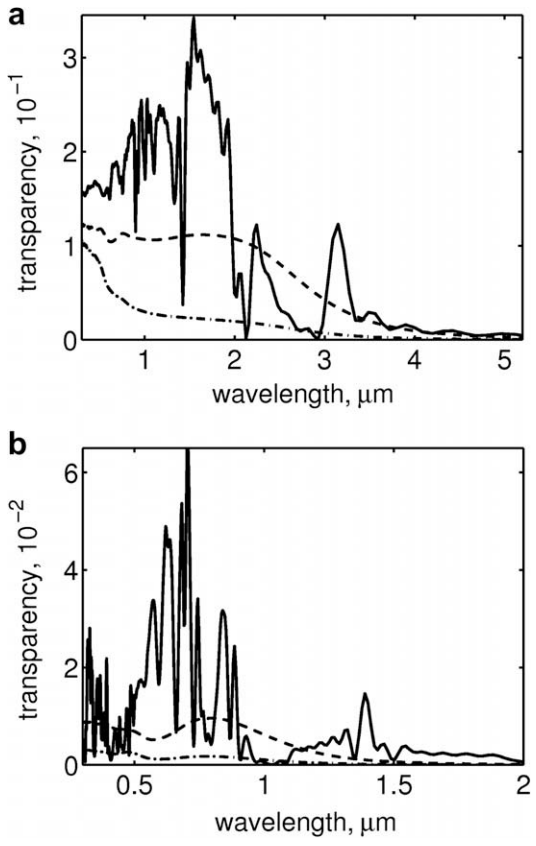

Fig. 3. Calculated transmission spectra of homogeneous square hole lattices (solid line), a single hole when light is collected by a monitor with 0.8 numerical aperture (NA) (dashed line) and with NA around 0.2 (dashed dotted line). (a) 0.8 μm hole size and (b) 300 nm hole size.

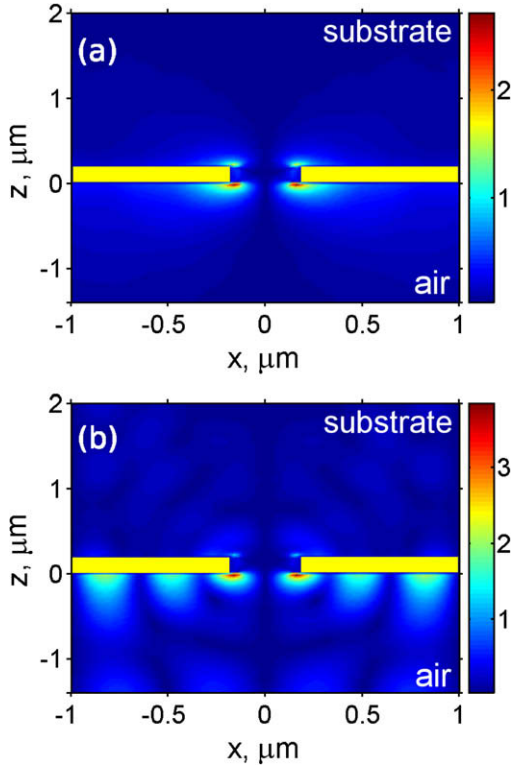

Fig. 4. Calculated amplitude distribution of the Z component of the electrical field for a single hole (a) and periodical lattice of holes (b). The cross section is made at the centre of hole. Light source is polarized along X, $\lambda = 0.7$ μm.

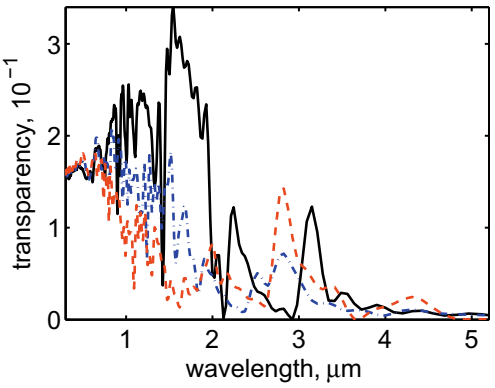

Fig. 5. 800 nm hole lattice: Transmission spectra with normal (solid line), 5° (dashed dotted line) and 10° (dashed line) angles of incidence.

resonances move to longer wavelengths with increasing the angle of incidence, while negative order effects go to shorter wavelengths. From our calculations we can see that the two last peaks of the spectrum near 2.3 and 3.2 μm move to shorter wavelengths and are therefore caused by negative order effects (Fig. 5 (dash-dotted and dashed lines) for angles of 5° and 10°, respectively). We can also say that peak shift to shorter wavelengths indicates the normal dispersion of the surface modes associated with these peaks [3].

From an experimental point of view it is also important to understand how the beam divergence would influence the transition spectrum of the nanohole array. We therefore, analyzed numerically the influence of small misalignments of the focal plane near the metal surface. For this purpose, we illuminated the sample with a diverging Gaussian beam and compared the transmission measurements with those of a plane wave. In particular, we illuminate the lattice of 800 nm holes by a Gaussian beam with a waist size of 1 μm or 2 μm and a focal plane placed at 1.4 μm from the metal surface. Our results shown in Fig. 6 reveal that the effect of beam divergence on the spectrum is mostly at short wavelengths, where the beam size obviously increases the total transmission through the holes. In general, however, the spectral features remain the same for the diverging beams.

Finally, we study how the film thickness changes the transmission spectrum. In Fig. 7 we compare the transmission spectra through the 800 nm nanohole lattice for metal films of 200 nm (solid line) and 100 nm (dashed dotted line) thickness. In agreement with previous studies [3], our results show that the change of the film thickness affects only slightly the position of the peak at 3.2 μm. The influence of the film thickness is mostly expressed in reduction of the intensity of the transmitted peaks with increasing of the thickness.

4. Quasi-periodic and chirped lattices

Last but not least, we investigate ways to engineer the properties of the perforated films by introducing quasi-periodicity of chirping of the lattice. Transmission through quasi- and aperiodic arrangements of holes in metallic films have been a subject of recent active interest [49–52]. This interest was motivated by the possibilities to tailor the transmission through the nanohole array. Such aperiodicity was usually found to broaden the transmission resonances over a wide spectral range [52]. However, for the purpose of our study, we are primarily interested in achieving sharp spectral features.

In our experiments we consider two types of nanohole structures: (i) a two-dimensional (2D) lattice with a one-dimensional (1D) quasi-periodic arrangement of the holes, and (ii) a 2D square lattice with constant periodicity, but with a 1D chirped size of the holes. In the first type of structure, we preserve the transmission properties of the isolated holes, however, the quasi-periodic arrangement influences the excitation of surface plasmons. An example of such a structure is the fabricated Thue–Morse sequence pattern as shown in the inset of Fig. 8a. The pattern is milled according to a binary sequence (01101001) where '1' is a milled pixel 300 × 300 nm and '0' is an opaque area. The sequence is repeated in vertical direction with period of 2 μm and in horizontal direction with period of 12 μm.

In the second type structure, we preserve the lattice periodicity (therefore the momentum matching in the transverse direction) while varying the size of the hole. Due to the hole size chirping we significantly modify the transmission properties of the individual apertures of the lattice. An example of such a structure is shown in the inset of Fig. 8b. It shows a lattice with the period of 2 μm and hole size varying in horizontal direction from 300 nm to 800 nm (50 nm change from one hole to another).

The measured transmission spectra of these two structures are shown in Fig. 8). For the quasi-periodic Thue–Morse pattern, the transmission spectrum does not show any sharp peaks of transmission, indicating the smearing of the transmission resonance in the monitored wavelength range. This is in good agreement with previous studies [52].

In the chirped structure, the transmission spectrum is also strongly modified, however some weaker transmission peaks can be observed between 0.9 μm and 1.1 μm. This measurement

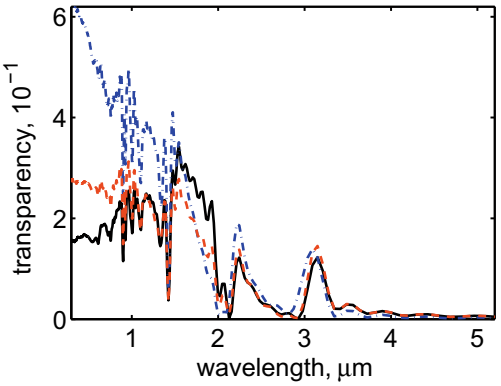

Fig. 6. Transmission through a 800 nm hole size lattice when the film is illuminated by a plane wave (solid line), Gaussian beam waist size 1 μm (dashed dotted line) and 2 μm (dashed line). Source focal planes are located at 1.4 μm from the gold surface.

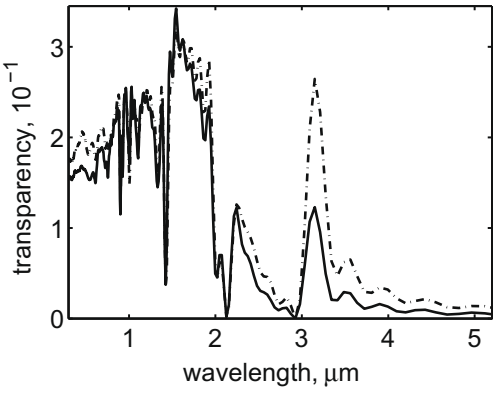

Fig. 7. Transmission through 800 nm hole size lattice on a gold film of thickness 200 nm (solid line) and 100 nm (dash-dotted line).

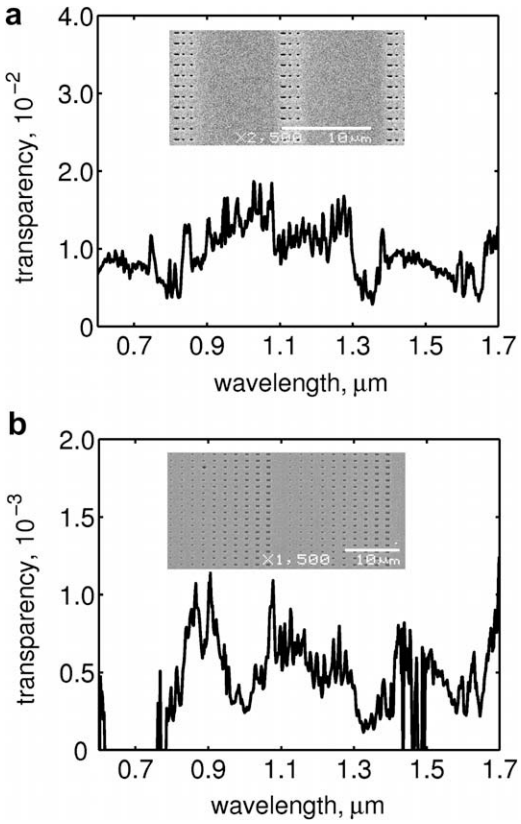

Fig. 8. Spectra of the Thue–Morse pattern (a) and size-chirped (b) nanoholes lattices (the signal between 0.6 and 0.8 μm is below noise level and not displayed). Insets – scanning electronic microscope images of the corresponded structures.

indicates that chirping of the hole size in the lattice of square apertures on a metal film provides a possible way to tailor the transmission spectrum through metal perforated films, however leads to the disappearance of any sharp transmission features observed in the strictly periodic lattices.

5. Conclusions

We have studied the transmission properties of nanohole lattices perforated in a gold film of thickness of 200 nm. In our experiments with square lattices of 800 nm holes and period of 2 μm, we have measured transmission around 1% and a flat spectrum in the region 0.6–1.7 μm. In contrast, in the experiments with the square lattices of 300 nm holes and the same period, we have observed a number of resonant transmission peaks at the wavelength ranges of 0.6–1.0 μm and 1.4–1.7 μm. The periodic arrangement of nanoholes leads to more than six fold enhancement of the transmission in comparison to the light transmitted through a single hole of the same size. Our experimental results are in a good qualitative agreement with the performed numerical FDTD calculations.

Finally, we have demonstrated a way to engineer the transmission through perforated metal films by inducing quasi-periodicity or chirping of the lattice by changing the size of individual holes. Such engineering may appear attractive for spectral filtering in spectroscopic and astronomical applications.

Acknowledgements

The authors would like to thank Dr. Vince Craig for the help with AFM images. This research is supported by the Australian Research Council. The Australian National Fabrication Facility and AMMRF, funded through Australian Government's National Cooperation Research Infrastructure Strategy, is gratefully acknowledged for access to the facilities.

References

[1] C. Genet, T.W. Ebbesen, Nature 445 (2007) 39.
[2] F.J. García de Abajo, Rev. Mod. Phys. 79 (2007) 1267.
[3] T.W. Ebbesen, H.J. Lezec, H.F. Ghaemi, T. Thio, P.A. Wolff, Nature 391 (1998) 667.
[4] W.H. Eggimann, R.E. Collin, Microwave Theory Tech. 10 (1962) 528.
[5] C.C. Chen, IEEE Trans. Microwave Theory Tech. 19 (1971) 475.
[6] R.C. McPhedran, G.H. Derrick, L.C. Botten, in: R. Petit (Ed.), Electromagnetic Theory of Gratings, Springer-Verlag, Berlin, 1980, p. 227.
[7] D.H. Dawes, R.C. McPhedran, L.B. Whitbourn, Appl. Opt. 28 (1989) 3498.
[8] A. Degiron, H.J. Lezec, W.L. Barnes, T.W. Ebbesen, Appl. Phys. Lett. 81 (2002) 4327.
[9] J.A. Porto, F.J. Garcia-Vidal, J.B. Pendry, Phys. Rev. Lett. 83 (1999) 2845.
[10] L. Martin-Moreno, F.J. Garcia-Vidal, H.J. Lezec, K.M. Pellerin, T. Thio, J.B. Pendry, T.W. Ebbesen, Phys. Rev. Lett. 86 (2001) 1114.
[11] E. Popov, M. Neviere, S. Enoch, R. Reinisch, Phys. Rev. B 62 (2000) 16100.
[12] A. Barbara, P. Quemerais, E. Bustarret, T. Lopez-Rios, Phys. Rev. B 66 (2002) 161403R.
[13] F.I. Baida, D. Van Labeke, Opt. Commun. 209 (2002) 17.
[14] A.K. Sarychev, V.A. Podolskiy, A.M. Dykhne, V.M. Shalaev, IEEE J. Quant. Elect. 38 (2002) 956.
[15] A.V. Zayats, L. Salomon, F. de Fornel, J. Microsc. 210 (2003) 344.
[16] P. Lalanne, J.C. Rodier, J.P. Hugonin, J. Opt. Pure Appl. Opt. 7 (2005) 422.
[17] Y. Takakura, Phys. Rev. Lett. 86 (2001) 5601.
[18] Y. Xie, A.R. Zakharian, J.V. Moloney, M. Mansuripur, Opt. Express 12 (2004) 6106.
[19] K.G. Lee, Q.-H. Park, Phys. Rev. Lett. 95 (2005) 103902.
[20] F. Marquier, J.-J. Greffet, S. Collin, F. Pardo, J.L. Pelouard, Opt. Express 13 (2005) 70.
[21] D.C. Skigin, R.A. Depine, Phys. Rev. Lett. 95 (2005) 217402.
[22] W.-C. Liu, D.P. Tsai, Phys. Rev. B 65 (2005) 155423.
[23] F.J. Garcia de Abajo, J.J. Saenz, I. Campillo, J.S. Dolado, Opt. Express 14 (2006) 7.
[24] H.T. Liu, P. Lalanne, Nature 452 (2008) 728.
[25] H.F. Ghaemi, T. Thio, D.E. Grupp, T.W. Ebbesen, H.J. Lezec, Phys. Rev. B 58 (1998) 6779.
[26] Z. Sun, Y.S. Jung, H.K. Kim, Appl. Phys. Lett. 83 (2003) 3021.
[27] W.L. Barnes, W.A. Murray, J. Dintinger, E. Devaux, T.W. Ebbesen, Phys. Rev. Lett. 92 (2004) 107401.
[28] K.J. Klein Koerkamp, S. Enoch, F.B. Segerink, N.F. van Hulst, L. Kuipers, Phys. Rev. Lett. 92 (2004) 183901.
[29] A. Degiron, T.W. Ebbesen, J. Opt. Pure Appl. Opt. 7 (2005) S90.
[30] R. Gordon, A.G. Brolo, A. McKinnon, A. Rajora, B. Leathem, K.L. Kavanagh, Phys. Rev. Lett. 92 (2004) 037401.
[31] Q.-J. Wang, J.-Q. Li, C.-P. Huang, C. Zhang, Y.-Y. Zhu, Appl. Phys. Lett. 87 (2005) 091105.
[32] A. Dechant, A.Y. Elezzabi, Appl. Phys. Lett. 84 (2004) 4678.
[33] D. Egorov, B.S. Dennis, G. Blumberg, M.I. Haftel, Phys. Rev. B 70 (2004) 033404.
[34] E. Altewischer, M.P. van Exter, J.P. Woerdman, J. Opt. Soc. Am. B 20 (2003) 1927.
[35] J. Bravo-Abad, A. Degiron, F. Przybilla, C. Genet, F.J. Garcia-Vidal, L. Martin-Moreno, T.W. Ebbesen, Nature Phys. 2 (2006) 120.
[36] H. Lezec, T. Thio, Opt. Express 12 (2004) 3629.
[37] H.F. Schouten, N. Kuzmin, G. Dubois, T.D. Visser, G. Gbur, P.F.A. Alkemade, H. Blok, G.W. 't Hooft, D. Lenstra, E.R. Eliel, Phys. Rev. Lett. 94 (2005) 053901.
[38] E. Laux, C. Genet, T. Skauli, T.W. Ebbesen, Nature Photon. 2 (2008) 161.
[39] H.A. Atwater, Scientific American 296 (2007) 56.
[40] M. Righini, G. Volpe, C. Girard, D. Petrov, R. Quidant, Phys. Rev. Lett. 100 (2008) 186804.
[41] K. Kneipp, H. Kneipp, I. Itzkan, R.R. Dasari, M.S. Feld, J. Phys.: Condensed Matter 14 (2002) 597.
[42] S. Kim, J. Jin, Y.-J. Kim, In-Y. Park, Y. Kim, S.-W. Kim, Nature 453 (2008) 757.
[43] J.A. Porto, L. Martín-Moreno, F.J. García-Vidal, Phys. Rev. B 70 (2004) 081402(R).
[44] G.A. Wurtz, R. Pollard, A.V. Zayats, Phys. Rev. Lett. 97 (2006) 057402.
[45] P. Marthandam, R. Gordon, Opt. Express 15 (2007) 12995.
[46] N. Garcia, M. Bai, Opt. Express 14 (2007) 10028.
[47] W. Dickson, G.A. Wurtz, P. Evans, D. O'Connor, R. Atkinson, R. Pollard, A.V. Zayats, Phys. Rev. B 76 (2007) 115411.
[48] H. Schouten, T. Visser, G. Gbur, D. Lenstra, H. Blok, Opt. Express 11 (2003) 371.
[49] T. Matsui, A. Agrawal, A. Nahata, Z.V. Vardeny, Nature 446 (2007) 517.
[50] S. Mei, T. Jie, L. Zhi-Yuan, C. Bing-Ying, Z. Dao-Zhong, J. Ai-Zi, Y. Hai-Fang, Chin. Phys. Lett. 23 (2006) 486.
[51] D. Pacifici, H.J. Lezec, L.A. Sweatlock, R.J. Walters, H.A. Atwater, Opt. Express 16 (2008) 9222.
[52] A. Gopinath, S.V. Boriskina, N.-N. Feng, B.M. Reinhard, L. Dal Negro, Nano Lett. 8 (2008) 2423.